



NH₄ClO₄ Decomposition with Nano–CuO, Cr₂O₃ and Mixed Catalysts

Rashmi Kumari¹ and M. R. R. Prasad^{2*}

1. Department of Nano Science and Technology, Central University of Jharkhand, Ranchi-835205, **INDIA**

2. Vikram Sarabhai space Centre, Thiruvananthapuram-695022, Kerala, **INDIA**

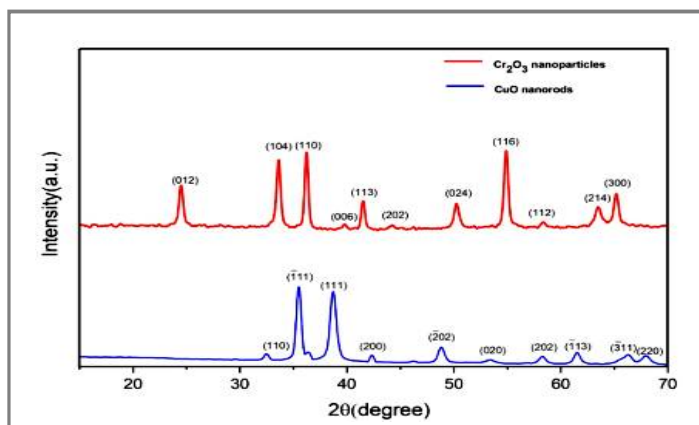
Email: mandapaka.p@gmail.com, rashmi809@gmail.com

Accepted on 14th May, 2020

ABSTRACT

Modification of thermal decomposition of ammonium per chlorate (AP) by Nano-Copper Oxide (CuO) and Nano-Chromium Trioxide (Cr₂O₃); and combinations of CuO and Cr₂O₃ are discussed. These studies were carried out employing XRD, FESEM, HRTEM, TG and DSC techniques. Presence of CuO or Cr₂O₃, or combinations of these oxides does not influence the endothermic crystallographic phase-transition temperature of AP from orthorhombic to cubic phase. Thermal stability of systems under consideration are in the order of: [AP: CuO: Cr₂O₃:: 100: 0.99: 0.01] > (AP–CuO) > [AP: CuO: Cr₂O₃:: 100: 0.995: 0.005] > [AP: CuO: Cr₂O₃:: 100: 0.98: 0.02] > (AP–Cr₂O₃) > AP. The catalyst system of [AP:CuO:Cr₂O₃:: 100:0.99: 0.01] gives maximum catalytic effect, and maximum enthalpy of 2131.9 J g⁻¹.

Graphical Abstract



XRD spectrum of CuO-nanorods; and Nano-Cr₂O₃.

Keywords: Ammonium per chlorate, Chromium Tri-oxide, Copper Oxide, Enthalpy, Mixed metal oxides.

INTRODUCTION

It is a well known fact that, Ammonium per chlorate (AP) is a widely used oxidizer in all composite solid rocket propellants (CSRPs). It is known that, in CSRPs, the maximum mass percentage of ingredients present is AP, and its thermal decomposition characteristics influence the combustion rates of CSRPs. Enhanced thermal decomposition of AP in the presence of CuO/MoS₂ composite and the catalytic mechanism were discussed by Hu *et al* [1]. Porous CuCo₂O₄ synthesized by template-free solution combustion method showed excellent catalytic activity on thermal decomposition of AP [2]. A simple method for controlling the morphology of CuO nano-structures by droplet technique was described by An *et al* [3]. Synthesis and its catalytic performance of porous Cr₂O₃ bead with 3D-continuous pore architecture on the thermal decomposition of AP were reported by Wang *et al* [4]. Hosseini *et al* [5] described the preparation, characterization and catalytic behavior of CuO nanoparticles on thermal decomposition of AP. Self-assembled CuO nano-architectures and their catalytic activity on the thermal decomposition of ammonium per chlorate was reported by Wang *et al* [6]. Effect of nano- CuO and Copper Chromite on the Thermal Decomposition of AP was reported by Patil *et al* [7]. Synthesis of chrysalis-like CuO nanocrystals and their catalytic activity on the thermal decomposition of ammonium per chlorate was studied by Wang *et al* [8].

Enhancing safety performance and thermal decomposition of AP through bio-inspired Copper - alginate was reported by Lu *et al* [9]. The mechanistic aspect of thermal decomposition of AP in the presence of CuO is discussed by Deepthi *et al* [10]. Catalytic decomposition of AP employing hollow mesoporous CuO microspheres was reported by Hu *et al* [11]. Thermal decomposition of AP catalyzed with CuO nanoparticles was reported by Elbasuney *et al* [12]. CuO nanoparticles supported on three-dimensional nitrogen-doped graphene as a promising catalyst for the thermal decomposition of AP was reported by Hosseinie *et al* [13]. Nano-particles of Cr₂O₃ obtained by combining wet mechanical milling technique with vacuum freeze-drying technology is efficient in accelerating the thermal decomposition of AP [14]. Thermal decomposition reaction mechanism of AP in the presence of KCl and Cr₂O₃ was elucidated by Burcat *et al* [15].

In the present study attention is focused towards understanding the role placed by cupric oxide, chromium trioxide and mixed metal oxides of CuO and Cr₂O₃.

MATERIALS AND METHODS

Materials: Copper (II) nitrate tri-hydrate [Cu (NO₃)₂·3H₂O]; and Chromium (III) nitrate nonahydrate [Cr (NO₃)₃ · 9H₂O] were purchased from Sigma Aldrich. Sodium hydroxide [NaOH] pellets were procured from M/s. Sd- fine chemicals limited and Ammonium per chlorate (AP) was received from the Ammonium per chlorate Experimental Plant (APEP) of Vikram Sarabhai Space Centre, Indian Space Research Organization (ISRO), Department of Space, Government of India. Nitrogen gas was of grade 1(99%) pure. Toluene was obtained from Finar Limited; and AR-grade ethanol was used. All chemicals were used without further purification.

Synthesis of CuO nanorods: CuO nanorods were synthesized through hydrothermal reaction, taking 0.12 g of Cu (NO₃)₂·3 H₂O in 5 mL of ethanol, with adequate stirring. Two grams of NaOH pellets were dissolved in 50 mL distilled water, and the resultant solution was transferred to 100 mL Teflon lined stainless steel autoclave, which was maintained at 140°C for 24 h. Subsequently, the autoclave was brought down to room temperature. The sample was dried to obtain CuO- nanorods.

Synthesis of Cr₂O₃ nanoparticles: 12 g of Cr (NO₃)₃·9H₂O was taken in 500 mL distilled water and stirred well till dissolution. During dissolution process, a few drops of ammonia solution were added to adjust the pH of the solution to 10 with continuous stirring till homogenization occurred. The precipitate so formed is allowed to stay overnight for settling down. The precipitate was centrifuged

with water and ethanol a number of times, and dried at 70°C for 2 h. The dried sample was calcined at 500°C for 5 h to get a green colored nano-Cr₂O₃.

Characterization: The as-prepared catalyst was analyzed using XRD (Bruker D-8) with monochromatic CuK α radiation ($\lambda=1.5406$) and its wavelength is comparable to the 'd' spacing with a step time of 0.7 s at room temperature. To know the morphology and topography, the catalyst was analyzed using FESEM (JEOL JSM 7610F) at a magnification of 10,000X to 30,000X. It shows a very clear image with low voltage and higher resolution as compared to SEM. In HRTEM the imaging of the sample was performed using Thermo Scientific (FEI) Talos F200X HRTEM. It is a specialized version of TEM and uses beam energy between 80-200kV with the magnification range of 50X to 1MX. For the thermal treatment of materials, TGA-TA Instruments SDT Q600 apparatus was used to study the thermal stability of the catalyst and the analysis of DSC was done using TA Instrument SDT DSC 250 to study the enthalpy of the samples. These were analyzed in the temperature between RT to 500°C with the heating rate of 10°C min⁻¹, under pure nitrogen gas flow at 50 mL min⁻¹.

RESULTS AND DISCUSSION

X-ray Diffraction Studies: The XRD spectrum obtained for CuO-nanorods, and Cr₂O₃-nanoparticles are shown in figure 1.

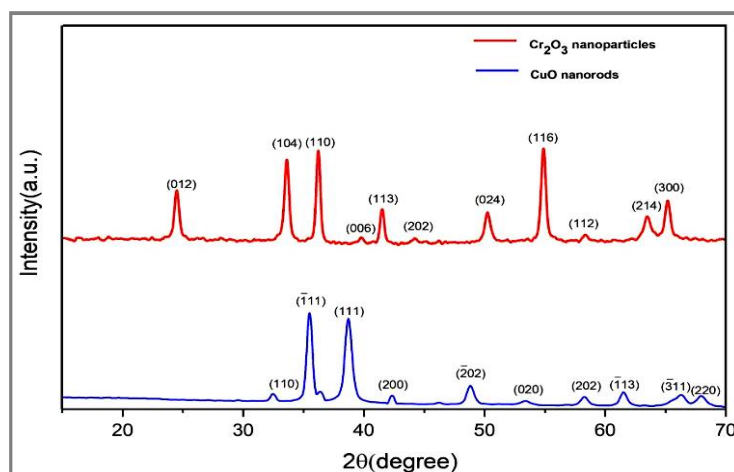


Figure 1. XRD spectrum of CuO – nanorods; and Nano -Cr₂O₃.

The SEM image of CuO-nanorods is shown in figure 2(a), and the HRTEM image is shown in figure 2(b). The SEM image of Cr₂O₃-nanoparticles is shown in figure 3(a), and the corresponding HRTEM image is shown in figure 3(b).

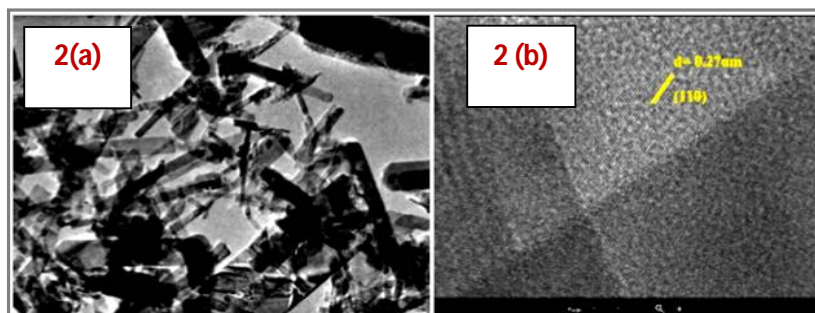


Figure 2(a). SEM Image of CuO-Nanorods, (b) HRTEM Image of CuO-Nanorods.

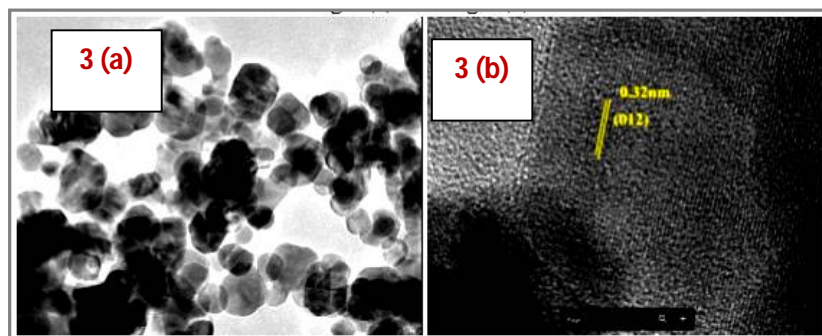


Figure 3(a). SEM Image of Cr_2O_3 -nanoparticles, 3(b) corresponding HRTEM Image.

Thermo gravimetric (TG) curves for pure AP, AP with CuO; and AP with Cr_2O_3 are shown in figure 4. The onset and end-set temperatures of decomposition and the temperature intervals are shown in table 1.

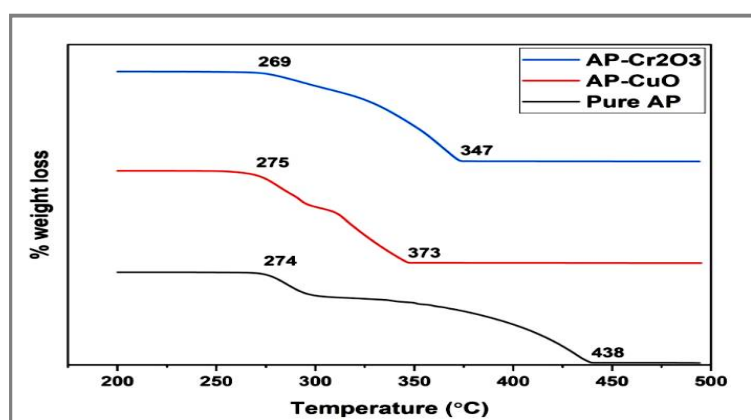


Figure 4. TG Curves of pure AP, AP – CuO; and AP – Cr_2O_3 Mixtures.

Table 1. Temperature Data from TG curves (Fig-4) of pure AP, AP – CuO; and AP – Cr_2O_3 Mixtures

Sample	Decomposition Temperatures (°C)		Temperature Interval (°C)
	Onset	End-set	
Pure AP	274	438	164
AP – CuO	275	373	98
AP – Cr_2O_3	269	347	78

From table 1, it can be seen that, the onset temperature of decomposition of AP in the presence of CuO is not affected, while in the case of AP- Cr_2O_3 system is marginally lowered. As far as the end-set temperatures are concerned, the order of thermal stability is AP > AP-CuO > AP- Cr_2O_3 . This is in tune with the observed temperature intervals of decomposition of these systems.

Differential Scanning Calorimetric (DSC) curves for pure AP, AP with CuO; and AP with Cr_2O_3 are shown in figure 5. crystallographic phase-transition temperature; enthalpy associated with the phase-transition; peak temperatures of low-temperature decomposition (LTD) and high-temperature decomposition (HTD); and total enthalpy release are tabulated in table 2.

From data in table 2, it can be inferred that, the presence of the catalyst has not influenced the crystallographic phase-transition temperature of AP from orthorhombic to cubic phase. The phase-transition enthalpy decreases in the order of Pure AP > AP-CuO > AP- Cr_2O_3 . The LTD peak has marginally shifted to a high temperature region in the case of AP-CuO and is unaffected in the case of

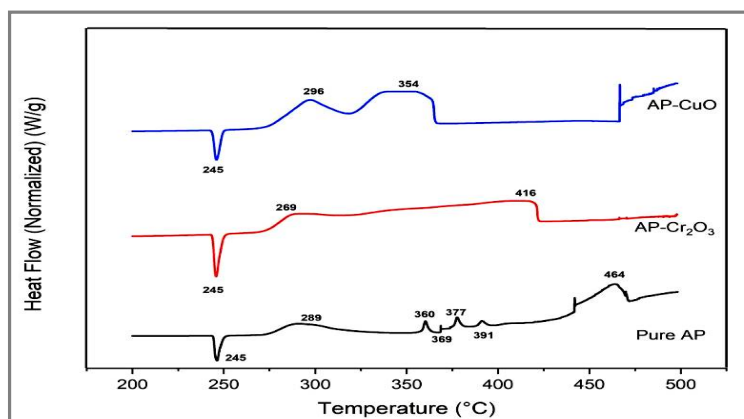


Figure 5. DSC Curves for pure AP, AP-CuO; and AP-Cr₂O₃ Mixtures.

Table 2. Kinetic Data from DSC curves (Fig 5), on thermal decomposition of pure AP, AP-CuO; and AP-Cr₂O₃ Systems

Sample	Endothermic Phase-Transition Temp. (°C)	Endothermic Enthalpy (J g ⁻¹)	Exothermic Decomp. Temp. (°C)		Total Enthalpy (J g ⁻¹)
			LTD	HTD	
Pure AP	246.3	114.6	289.5	463.6	739.1
AP – CuO	246.0	104.5	296.2	355.1	2031.4
AP – Cr ₂ O ₃	245.8	87.9	287.8	417.8	1499.2

LTD = Low-temperature Decomposition, HTD = High-temperature Decomposition

AP-Cr₂O₃ system. However, in the case of HTD peak temperatures, the shift is in the order of pure AP > AP- Cr₂O₃ > AP- CuO system. The temperature intervals are 58.9°C, 130°C, and 174.1°C, for AP-CuO, AP-Cr₂O₃, and pure AP, respectively. From the total exothermic heat release considerations, the heat release is 2.75 times more for AP-CuO system (2031 J g⁻¹); and 2.03 times more for AP-Cr₂O₃ system (1499.2 J g⁻¹) when compared with pure AP. This could be explained on the lines that, the melting temperatures of CuO is of the order of 1201°C, and that for Cr₂O₃ is of the order of 2435°C. From the melting temperatures of these oxides, it can be inferred that, Cr₂O₃ acts as a greater heat sink material than CuO. Thus, we can conclude that, CuO is a better catalyst system releasing maximum energy.

The TG curves for AP decomposition in the presence of mixed catalyst system of CuO and Cr₂O₃, where in the ratio between CuO and Cr₂O₃ is varied, is presented in figure 6. Both the onset and end-set temperatures, and the temperature intervals of decomposition of AP in the presence of these mixed oxides is presented in table 3.

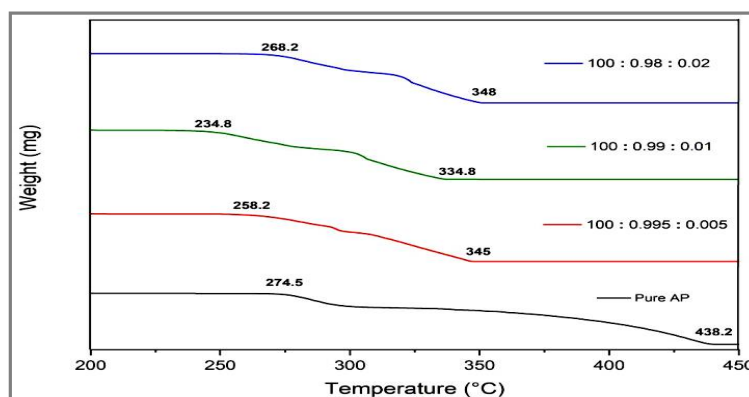


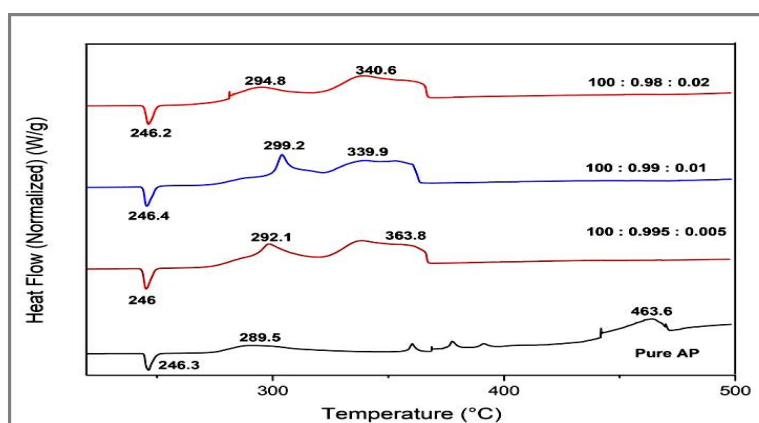
Figure 6. TG Curves of AP in the presence of mixed catalysts of CuO and Cr₂O₃ in different ratio combinations.

Table 3. Onset and end-set temperatures of decomposition, and temperature interval of decomposition of AP in the presence of mixed catalysts of CuO and Cr₂O₃ in different ratio combinations

Sample System	Decomposition Temperature (°C)		Temperature Interval (°C)
	Onset	End-set	
Pure AP	274.5	438.2	163.7
AP: CuO; Cr ₂ O ₃ ::100: 0.995: 0.005	258.2	345.0	86.8
AP: CuO; Cr ₂ O ₃ ::100: 0.99: 0.01	234.8	334.8	100.0
AP: CuO; Cr ₂ O ₃ ::100: 0.98: 0.02	268.2	348.0	79.8

From table 3, it can be noticed that, as the concentration of Cr₂O₃ is increased from 0.005 to 0.01, both the onset and end-set temperatures of decomposition decrease, indicating the catalysis of both the low-temperature decomposition (LTD) and high-temperature decomposition (HTD) of AP. Subsequent increase in Cr₂O₃ content to 0.02, there is a tendency of reversing the decomposition process.

The DSC curves for AP decomposition in the presence of mixed catalyst system of CuO and Cr₂O₃, where in the ratio between CuO and Cr₂O₃ is varied, is presented in figure 7. The endothermic crystallographic phase-transition temperature for the transition from orthorhombic to cubic phase and the associated energy absorbance; the temperature at maximum peak rate of decomposition with respect to LTD and HTD of AP; and the associated total enthalpy release are presented in table 4.

**Figure 7.** DSC Curves of AP in the presence of mixed catalysts of CuO and Cr₂O₃ in different ratio combinations.**Table 4.** Kinetic data for the thermal decomposition of AP in the presence of mixed catalysts of CuO and Cr₂O₃ in different ratio combinations

Sample System of AP:CuO:Cr ₂ O ₃	Endothermic Phase – transition		LTD	HTD	Total heat release (J g ⁻¹)
	Temp.(° C)	Enthalpy Change (J g ⁻¹)	Temp. (° C)	Temp. (° C)	
100:0.995:0.005	246.0	105.9	292.1	363.8	2017.1
100: 0.99: 0.01	246.4	111.3	299.2	339.9	2131.9
100: 0.98: 0.02	246.2	97.2	294.8	340.6	1930.9
Pure AP	246.3	114.6	289.5	463.6	739.02

From the data in table 4, the following inferences can be made:

- The addition of CuO-Cr₂O₃ mixed catalyst system to AP has no influence on its phase-transition temperature, as well as, on the endothermic enthalpy change, except for the system where the ratio of Cr₂O₃ is 0.02. In this case, there is a considerable enthalpy change attributable to the greater heat sink capability of Cr₂O₃ (based on relative melting points of these oxides).

- With respect to LTD of AP, there is a marginal shift towards higher temperature region with changes in the ratio of CuO: Cr₂O₃, which is not appreciable.
- With respect to HTD of AP, there is a considerable influence of the mixed catalyst system as the ratios between CuO: Cr₂O₃ change, indicating the mixed catalyst system catalyzes the HTD of AP. However, at CuO: Cr₂O₃ ratios of 0.99:0.01 and 0.98:0.02, there is no change in the peak rate of decomposition temperature, indicating the saturated condition.
- In terms of total energy release, the AP: CuO: Cr₂O₃ at the ratio of 100: 0.99: 0.01 maximum heat release (2131.9 J g⁻¹) is obtained. This combination proves to be the best system for catalysis of AP decomposition.

APPLICATION

These studies have utility in modifying the combustion rates of composite solid rocket propellants.

CONCLUSION

In the presence of single nano-catalyst system, AP-CuO system gives maximum heat release of 2031.4 J g⁻¹. In the case of mixed transition metal oxide systems, AP: CuO: Cr₂O₃::100: 0.99: 0.01 gives maximum heat release of 2131.9 J g⁻¹.

ACKNOWLEDGEMENT

The authors wish to express their gratitude to the authorities at Vikram Sarabhai Space Centre, Thiruvananthapuram-695022, Kerala and Indian Institute of Chemical Technology (IICT), Hyderabad -500007, Telangana for their support and encouragement in this research activity.

REFERENCES

- [1]. Y. Hu, Y. Yang, R. Fan, K. Lin, D. Hao, D. Xia, P. Wang, Enhanced Thermal Decomposition Properties and Catalytic Mechanism of Ammonium Per chlorate over CuO/MoS₂ Composite, *Applied Organometallic Chemistry*, **2019**, 33(9), e5060
- [2]. X. Xiao, Z. Zhang, L. Cai, Y. Li, Z. Yan, Y. Wang, The excellent catalytic activity for thermal decomposition of ammonium per chlorate using porous CuCo₂O₄ synthesized by template-free solution combustion method", *Journal of Alloys and Compounds*, **2019**, 797, 548-557.
- [3]. H. R. An, F. S. Cai, X. W. Wang, Z. Yuan, A Simple Method for Controlling the Morphology of CuO Nanostructures by Droplet, *Advanced Engineering Materials II; Advanced Materials Research*, **2012**, 535-537, 280-283
- [4]. D. Wang, Y. Jiang, Y. Hu, D. Hao, Y. Yang, R. Fan, D. Xia, K. Lin, Porous Cr₂O₃ bead with a 3D continuous pore architecture: synthesis and its catalytic performance for decomposition of ammonium per chlorate, *New J. Chem.*, **2019**, 43(26), 10560-10566
- [5]. S. G. Hosseini, E. Ayoman, A. Kashi, Preparation, characterization and catalytic behavior of copper oxide nanoparticles on thermal decomposition of ammonium per chlorate particles, *Particulate Science and Technology*, **2018**, 36(6), 751-761.
- [6]. J. Wang, S. He, Z. Li, X. Jing, M. Zhang, Z. Jiang, Self-assembled CuO nano-architectures and their catalytic activity in the thermal decomposition of ammonium per chlorate, *Colloid Polym. Sci.*, **2009**, 287, 853-858
- [7]. P. R. Patil, V. N. Krishnamurthy, S. S. Joshi, Effect of Nano-Copper Oxide and Copper Chromite on the Thermal Decomposition of Ammonium Per chlorate, *Propellants, Explosives, Pyrotechnics*, **2008**, 33 (4), 266-270.
- [8]. J. Wang, S. He, Z. Li, X. Jing, M. Zhang, Z. Jiang, Synthesis of chrysalis-like CuO nanocrystals and their catalytic activity in the thermal decomposition of ammonium per chlorate, *J. Chem. Sci.*, **2009**, 121(6), 1077-1081.

- [9]. Y. Lu, J. Chen, R. Wang, P. Xu, X. Zhang, B. Gao, C. Guo, G. Yang, Bio-inspired Cu-alginate to smartly enhance safety performance and the thermal decomposition of ammonium per chlorate, *Applied Surface Science.*, **2019**, 470, 269-275
- [10]. L. S. Deepthi, T. Deepthi, M. S. Haseena, T. Jayalatha, G. Rocha Krishnan, Salu Jacob, R. Rajeev, Insight into the catalytic thermal decomposition mechanism of ammonium per chlorate, *J. Therm Anal Calorim*, **2019**, 138(1), 1-10.
- [11]. Y. Hu, S. Yang, B. Tao, X. Liu, K. Lin, Y. Yang, R. Fan, D. Xia, D. Hao, Catalytic decomposition of ammonium per chlorate on hollow mesoporous CuO microspheres, *Vacuum*. **2019**, 159, 105-111.
- [12]. S. Elbasuney, M. Yehia, Thermal Decomposition of ammonium per chlorate catalyzed with CuO nanoparticles, *Defence Technology*. March, **2019**.
- [13]. S. G. Hosseini, Z. Khodadaipoor, M. Mahyari, CuO nanoparticles supported on three-dimensional nitrogen-doped graphene as a promising catalyst for thermal decomposition of ammonium per chlorate, *Applied Organometallic Chemistry*, **2018**, 32(1), e3959.
- [14]. G. Hao, L. Xiao, Y. Hu, F. Shao, X. Ke, J. Liu, F. Li, W. Jiang, F. Zhao, Gao, Facile preparation of Cr₂O₃ nanoparticles and their use as an active catalyst on the thermal decomposition of ammonium per chlorate, *Journal of Energetic Materials*, **2019**, 37(3), 251-269.
- [15]. A. Burcat, B. Carmon, M. Steinberg, A study on the mechanism of the thermal decomposition of ammonium per chlorate, *Israel Journal of Chemistry*, **1968**, 6(6), 859-864.